Monte Carlo characterization of photoneutrons in the radiation therapy with high energy photons: a Comparison between simplified and full Monte Carlo models

H. Ghiasi[1] and A. Mesbahi[1,2*]

[1]Medical Physics Department, Medical School, Tabriz University of Medical Sciences, Tabriz, Iran
[2]Radiation Oncology Department, Imam Hospital, Daneshgah Street, Tabriz, Iran

Background: The characteristics of secondary neutrons in a high energy radiation therapy room were studied using the MCNPX Monte Carlo (MC) code. ***Materials and Methods:*** Two MC models including a model with full description of head components and a simplified model used in previous studies were implemented for MC simulations. ***Results:*** Results showed 4-53% difference between full and with the simplified model in the neutron fluence calculation. Additionally, in full MC model, increase in the field size decreased the neutron fluence but for simplified model, increase in the field size led to increase in neutron fluence. In calculating the neutron and capture gamma ray dose equivalent, simplified model overestimated (9-47%) and (20-61%) respectively in comparison to the full simulated model. However, a close agreement was seen between two models, for field size of 10×10 cm². ***Conclusion:*** for MC modeling of photoneutrons and capture gamma in radiotherapy rooms, the detailed modeling of linac head instead of simplified model is recommended. **Iran. J. Radiat. Res., 2010; 8 (3): 187-193**

Keywords: *Photoneutron, capture gamma rays, Monte Carlo simulation, Linac head modeling.*

INTRODUCTION

Application of high energy photon beams has been joined with the production of the secondary neutrons [1, 2]. Neutrons are produced through (γ,n) photonuclear interactions within the head of linac, patient body and the walls of treatment room [3]. Produced neutrons (photoneutrons) are electrically uncharged and for this reason interaction between photoneutrons and materials is less than charged particles such as electron, protons and other charged particles. Photoneutrons are not being absorbed intensively like charged particles. Otherwise, they are able to penetrate in different materials, reach to the high distances, pass through the head of linac shielding and finally contaminate the room and its maze. International Commission on Radiological Protection (ICRP) report No.103 has appointed high values of radiation weighting factor (W_R) for photoneutrons that presents the biological effects of photoneutrons produced in the radiation therapy with high energy photons [4]. Also, (γ,n) photonuclear reaction energy threshold depends on the material's atomic number (Z) and increasing the Z, decreases the energy threshold [5]. This threshold is around 8 MeV for high Z materials such as W whilst for low Z materials such as C and O is 18 MeV and 16 MeV respectively. The cross-section of the reaction increases with increasing in the Z and for high Z materials is around 50 times lower than low Z ones (400 mbarn for W and 8 mbarn for C) [6-8]. The linac head assembly consists of high Z materials for shielding against photons, but it also was recommended that for the linacs operating above 10 MV, shielding against photoneutrons must be considered as well as photons [5].

In Monte Carlo (MC) studies on the secondary neutrons [9-13] researchers used two models of the head for photoneutron calculations including full modeling of linac head which simulated all detailed components of the linac head and the simplified

*Corresponding author:
Dr. Asghar Mesbahi,
Medical physics department, Medical school, Tabriz university of Medical Sciences, Tabriz, Iran.
Fax: +98 411 3364660
E-mail: amesbahi2010@gmail.com

model. The simplified model of the linac head consisted of a spherical tungsten shell with thickness of 10 cm and a conical aperture for opening the desirable radiation field size. An isotropic source with spectra derived from below equation was located at the centre of the tungsten sphere.

$$\frac{dN}{dE_n} = \frac{0.8929 \ E_n}{(T)^2} \ \exp \ (\frac{-E_n}{T}) + \frac{0.1071 \ Ln \ [E_{max}/(E_n + 7.34 \ ) \ ]}{\int_0^{E_{max}-7.34} Ln \ [\ E_{max}/(E_n + 7.34 \ ) \ ] \ dE_n} \quad (1)$$

In this equation, first part describes the evaporation of photoneutrons and second part shows direct emission of photoneutrons. T in equation 1 is the nuclear temperature in MeV, E_n is neutron energy and E_{max} is maximum energy of the incident photon. The simplified model has applied to study and evaluate the neutron contamination in the radiation therapy rooms with high energy X-rays. Some other researches have been done with full simulation of the linac head [9, 14-18]. On the other hand, accurate knowledge about secondary neutrons characteristics can help to the improvement of shielding accuracy and better radiation protection of patients and staff. Thus, in the current study, the characteristics of the secondary neutrons were studied with both full simulation of the linac head and simplified model. Also, a comparison was made between the results of two models.

MATERIALS AND METHODS

Monte Carlo simulation

The MCNPX MC code (Version. 2.4.0) was used for our simulations [19]. The MCNP4X is a general purpose MC code that can transport electron, photon, and photoneutron and coupled electron-photon-photoneutron. The code treats an arbitrary 3-dimantional configuration of materials in geometric cells bounded by first and second degree and forth degree elliptical tori.

Varian 2100 C/D Clinac with photon beam of 18 MV was simulated using the linac manufacture provided data. Main

parts of the linac those were simulated are primary electron source, target, container, primary collimator, movable jaws, bending magnet, flattening filter and lead shielding assembly of head. A 50×50×50 cm³ water phantom at the source to surface distance of 100 cm was simulated in the both models. A typical radiation therapy room with the dimension of 12.7×11×4.2 m³ made of ordinary concrete with the density of 2.35 gr/cm³, recommended by the NCRP No. 144 was simulated [20]. Composition of the simulated concrete was 0.013 Hydrogen, 1.165 Oxygen, 0.737 Silicon, 0.194 Calcium, 0.04 Sodium, 0.006 Magnesium, 0.107 Aluminum, 0.003 Sulfur, 0.045 Potassium and 0.029 Iron (figure 1). Direction of the primary radiation was simulated in downward orientation.
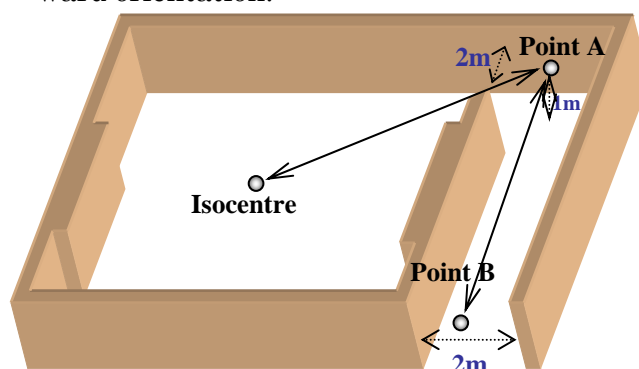

Figure 1. Simulated treatment room geometry and points A and B where the neutron and capture gamma calculations were performed.
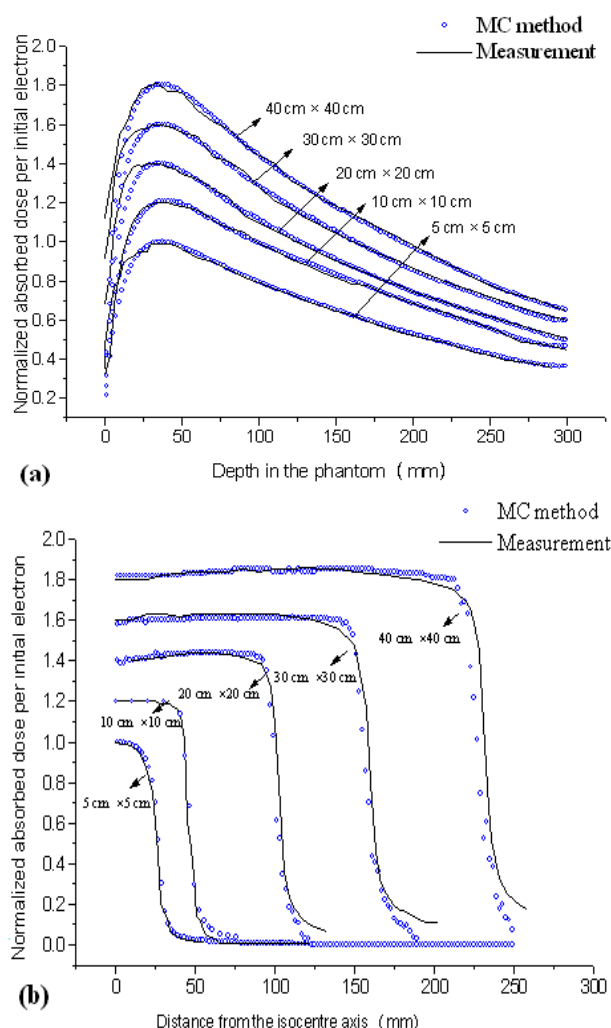
Calibration of the full simulated model

After the simulation of Varian 2100 Clinac, tuning the primary electron beam energy was performed by the steps of 0.1 MV and this value was set to be 18.1 MV [21-25]. For speeding up the calculations, BNUM value in the phys card of input file was changed and the optimum value was chosen. BNUM in input file determines the number of photons produced per incident electron on target used for X-ray production. Running the program in constant time (5 min), photon fluence was calculated over a simulated cylindrical cell positioned at 1 cm below the flattening filter. The BNUM value that caused the minimum statistical error for the fluence calculation was set as value

of the BNUM in the simulation program (figure 2). The optimum value was set to be 5. It is seen from figure 2 that optimizing the BNUM value decreased the statistical error in the calculation of fluence from 0.78% in the default value to 0.53% in the optimized value.
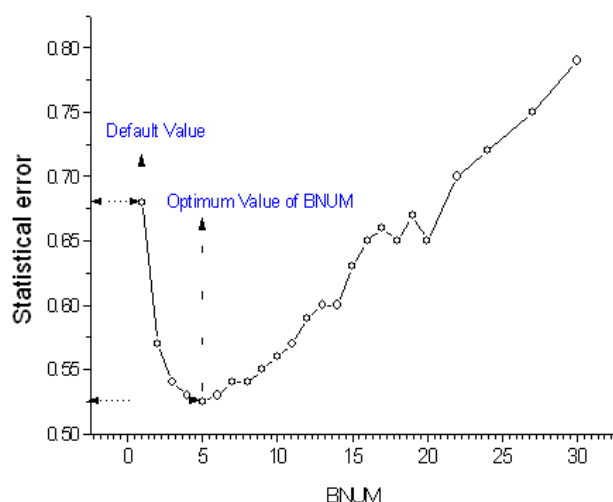
Figure 2. Variation of statistical error of results with different BNUMs.

Calibration of full model was carried out by comparison of the percent depth dose (PDD) and beam profiles in different field sizes and was shown in figure 3. For finding the neutron source strength, Q_N of simulated linac, that represents the number of produced photoneutrons when linac delivers 100 cGy photon dose to the isocentre [20, 26], a spherical surface with its center at the centre of target and with the radius of 100 cm was simulated according to the McGinley and Lundry method [27]. Applying the F2 tally that scores the number of particles over a surface, number of produced photoneutrons per initial electron was obtained. Using the F6 tally that calculates deposited energy (MeV) per gram of material, absorbed dose from photons at the isocenter per initial electron was obtained. Using these values, the number of 1.3×10^{12} neutrons per absorbing 100 cGy of X at the isocentre was obtained and this value was the Q_N or neutron source strength of the model.

Figure 3. Comparison the results of MC and Measurements for calibration the full simulated model. a) PDDs in different field sizes obtained from the MC method and measurement. b) beam profiles in different field sizes obtained from the MC method and measurement.

Description of the simplified model

Simple model of linac head was simulated as a tungsten shell with inner radius of 10 cm and outer radius of 15 cm with a conical aperture to create the desirable radiation field. The photoneutron spectra derived from full simulated linac head was positioned at the centre of tungsten spherical cell. Because of high radiation attenuation characteristics of tungsten rather than other materials such as iron and lead, simple model of head was simulated with tungsten. Figure 4 shows the simulated simple model for linac head.
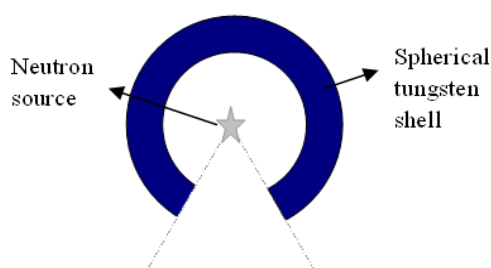
Figure 4. The geometry of simulated simple model of linac head.

Fluence and spectra at the isocentre for different field sizes

To obtain the spectra and total fluence at the isocentre, a 5 cm diameter water cell was simulated at the isocentre. Using F4 tally (scores the transmitted particle over a cell) in small energy bins, total neutron fluence and neutron fluence was scored for field sizes of 10×10 cm^2, 20×20 cm^2 and 40×40 cm^2. Statistical error in all of the energy bins was less than 2%. Table 1 shows the total neutron fluence at the isocentre for both models. This calculation was carried out for the both the full and simplified

Figure 5. Neutron spectra at the isocenter for 10×10, 20×20 and 40×40 cm^2. a) spectra were derived from simplified model of the linac head. b) Spectra was derived from full simulated head of linac.

model. The spectra from both models were shown in the figure 5.

Neutron and capture gamma dose equivalent in the maze

when secondary neutrons interact with the materials, through (n,γ) photonuclear reaction, photons with the energies from 3.5 MeV to around 10 MeV was released within short mazes [26]. To calculate the neutron and capture gamma dose equivalent, two spherical water cells with the diameter of 10 cm were simulated at the points of A and B as seen in figure 1. The Q_N of 1.3×10^{12} nGy^{-1} was also used for simplified model of linac [12]. Neutron and capture gamma ray dose per Gy X-ray at the isocentre was calculated at points A and B. Then, by applying the recommended W_R[4], the neutron dose in terms of Gy was converted to the dose equivalent in terms of Sv.

RESULTS AND DISCUSSION

Figure 3 shows the MC calculated and measured PDDs and beam profiles for different field sizes (5×5, 10×10, 20×20, 30×30 and 40×40 cm^2). In the percentage depth dose and beam profile calculations, maximum difference between measurement and MC results was seen in the build up regions of PDD curves. It was 11%, 1.8% at the build up and the descending part respectively. For beam profiles, in flat region the difference was 1.6%, and reached to 5% at the penumbra region and in the out of field region was 11%. The results were in accordance with the previous studies on MC modeling of linacs [21-23, 28].

Using the McGinley and Lundry method for calculating Q_N, the value of 1.3×10^{12} nGy^{-1} was obtained for our model. This value was close to the Mao *et al.* reported value of 1.2×10^{12} nGy^{-1} and was 7.6% higher [12]. Also, Followill *et al.* reported the Q_N of this value for same linac as 0.96×10^{12} nGy^{-1} for the same linac using measurements [29]. This value showed 26% difference with our calculated value. These

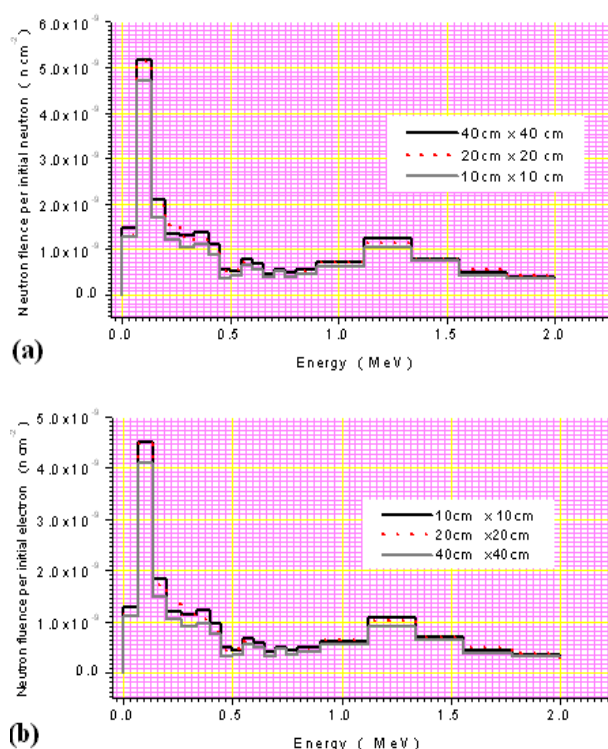differences in the Q_N value can be attributed to the modeling accuracy, primary electrons energy and method of calculation and also uncertainties associated with neutron measurement methods.

Total fluence of the photoneutrons at the isocentre for 10×10 cm^2 was obtained as $1.83\times10^7\pm2.78\times10^6$ ncm^{-2}Gy^{-1} X for the full MC model and this value for simplified model was $1.74\times10^7\pm2.78\times10^6$ ncm^{-2}Gy^{-1}X. Using a simplified model, Zabihzadeh *et al.* obtained the value 1.07×10^7 n cm^{-2}Gy^{-1}X for photoneutron fluence at the isocenter [30]. Figure 5 shows the spectra, derived from both full and simplified model in 10×10 cm^2, 20×20 cm^2 and 40×40 cm^2 field sizes. It is seen that for all of field sizes, the shape of the spectra remains constant. Table 2 shows the neutron fluence in different field sizes per Gy X-ray at the isocenter.

It was seen from table 2 that there is a contrast between two models considering the relation between field size and neutron fluence. This reverse behavior may be due to the effect of simplifications in MC modeling. In the simplified model interactions between the photons and some components

of the head including the flattening filter and primary collimator were neglected. Number of interactions and the direction of photon scattering vary significantly with the jaws movement in full model. In the simplified model, opening the aperture increases the neutron fluence and there is no other possibility for photon-material interaction in the linac head. Sohrabi and Mostofizadeh, reported that neutron dose increases with decreasing in the field size using measurements with the Polycarbonate film dosimetry [31]. Mesbahi *et al.* and Gavami *et al.* also reported the same results with full simulation of the head [32,33]. Higher values in the simplified model can be attributed to the simple spectra that was derived from equation 1, but for full simulated model, the spectra was derived from the full model of the head and very low energies also participated in the spectra. In the table 3 capture gamma dose equivalent in three field sizes resulted from both models was shown. It is seen that simplified model, overestimates the gamma ray dose equivalent for all field sizes. Using high energy neutrons in the spectra used for the

Table 1. Neutron fluence at the isocentre (in n cm^{-2}) per Gy X-ray for both models used in the current study.

Field size (cm^2)	Simple model	Full model	Difference (%)
10×10	$1.74\times10^7\pm2.78\times10^6$	$1.83\times10^7\pm2.78\times10^6$	4
20×20	$2.11\times10^7\pm3.27\times10^6$	$1.35\times10^7\pm2.26\times10^6$	36
40×40	$2.30\times10^7\pm3.71\times10^6$	$1.07\times10^7\pm1.78\times10^6$	53

Table 2. Neutron dose equivalent at the maze entrance (in mSv/Gy X).

Field size (cm^2)	Simple model	Full model	Difference (%)
10×10	$3.60\times10^{-4}\pm6.12\times10^{-6}$	$3.25\times10^{-4}\pm5.35\times10^{-6}$	9
20×20	$3.46\times10^{-4}\pm5.88\times10^{-6}$	$2.59\times10^{-4}\pm4.45\times10^{-6}$	25
40×40	$4.18\times10^{-4}\pm7.40\times10^{-6}$	$2.19\times10^{-4}\pm3.88\times10^{-6}$	47

Table 3. Capture gamma dose equivalent at the maze entrance for both MC models (in mSv/Gy X).

Field size (cm^2)	Simple model	Full model	Difference (%)
10×10	$1.97\times10^{-4}\pm3.95\times10^{-6}$	$1.57\times10^{-4}\pm2.65\times10^{-6}$	20
20×20	$2.23\times10^{-4}\pm3.82\times10^{-6}$	$9.84\times10^{-5}\pm1.95\times10^{-6}$	77
40×40	$2.41\times10^{-4}\pm3.97\times10^{-6}$	$9.38\times10^{-5}\pm1.05\times10^{-6}$	61

simplified model may cause these differences. From tables 1, 2 and 3 it can be deduced that for the reference field size of 10×10 cm² there was a good agreement between two models but for other field sizes differences between two models increase.

Considering the data shown in table 2 and 3, it is revealed that the application of simple spectra derived from equation 1 leads to overestimation in neutron and capture gamma dose. On the other hand, we think that using the simplified model results in removing real physical effects associated with jaws movement. However, our results showed that in spite of observed differences between simple and full MC models, the simplified model can be used as reliable estimator for neutron dose calculations in reference field size of 10×10 cm².

CONCLUSION

In the current study the impact of different MC modeling of linac head for neutron dose calculations was evaluated by MCNPX MC code. Results indicated that the simplified model is capable to calculate neutron and capture gamma dose or fluence in the reference field size, but it can't describe the effect of variations in parameters such as field size on the fluence and dose. In the reference field size, simple model and full simulated model of linac head show close agreement in photoneutron characteristics. But, in the other field sizes, results showed a considerable difference between two models that may lead to inaccurate calculations. Finally, in order to have more accurate calculation for neutrons, application of the full MC model used in our study instead of simple MC model for shielding calculations is recommended.

REFERENCES

1. International Atomic Energy Agency (IAEA) (2006) Radiation protection in the design of radiotherapy facilities. *Safety Reports series No. 47* .
2. Attix FH, Rank EX, August LS, Miller GE, Shapiro P (1976) A shielding maze at a neutron radiotherapy facility. *Health Phys,* **31:** 78-80.
3. Allen PD and Chaudhri MA (1982) The dose contribution due to photonuclear reactions during radiotherapy. *Med Phys,* **9:** 904-906.
4. ICRP Publication 103 ((2007 Recommendations of the international commission on radiological protection. (Oxford: Elsevier) *Ann ICRP, 37 (2-3).*
5. National Council on Radiation Protection and Measurements (2005) Structural shielding design and evaluation for megavoltage X-ray and gamma-ray radiotherapy facilities. NCRP No. **151**, Washington, DC, pp. 1-246 .
6. Lin JP, Chu TC, Lin SY, Liu MT (2001) The measurement of photoneutrons in the vicinity of a Siemens Primus linear accelerator. Appl Radiat Isot, 5.321-315 :5
7. Zanini A, Durisi E, Fasolo F, Visca L, Ongaro C, Nastasi U, Burn KW, Annand JR (2004) Neutron spectra in a tissue equivalent phantom during photon radiotherapy treatment by LINACS. *Radiat Prot Dosimetry,* **110:** 157-160.
8. Zanini A, Fasolo F ,Visca L, Durisi E, Perosino M, Annand JR, Burn KW (2005) Test of a bubble passive spectrometer for neutron dosimetry. *Phys Med Biol,* **50:** 4287-4297.
9. Chibani O and Ma CM (2003) Photonuclear dose calculations for high-energy photon beams from Siemens and Varian linacs. *Med Phys, 30: 1990-2000.*
10. Kase KR, Mao XS, Nelson WR, Liu JC, Kleck JH, Elsalim M (1998) Neutron fluence and energy spectra around the Varian Clinac 2100C/2300C medical accelerator. *Health Phys,* **74:** 38-47.
11. Lin JP, Liu WC, Lin CC (2007) Investigation of photoneutron dose equivalent from high-energy photons in radiotherapy. *Appl Radiat Isot, 65: 599-604.*
12. Mao XS, Kase KR, Liu JC, Nelson WR, Kleck JH, Johnsen S (1997) Neutron sources in the Varian Clinac 2100C/2300C medical accelerator calculated by the EGS4 code. *Health Phys,* **72:** 524-529.
13. Waller EJ, Jamieson TJ, Cole D, Cousins T, Jammal RB (2003) Experimental and computational determination of neutron dose equivalent around radiotherapy accelerators. *Radiat Prot Dosimetry,* **107:** 225-232.
14. Al-Ghamdi H, Fazal UR, Al-Jarallah MI, Maalej N (2008) Photoneutron intensity variation with field size around radiotherapy linear accelerator 18-MeV X-ray beam. *Radiation Measurements,* **43:** S495-S499.
15. Becker J, Brunckhorst E, Schmidt R (2007) Photoneutron production of a Siemens Primus linear accelerator studied by Monte Carlo methods and a paired magnesium and boron coated magnesium ionization chamber system. *Phys Med Biol,* **52:** 6375-6387.
16. Facure A, da Silva AX, Falcao RC (2007) Monte Carlo simulation of scattered and thermal photoneutron fluences inside a radiotherapy room. *Radiat Prot Dosimetry,* **123:** 56-61.
17. Facure A, da Silva AX, Falcao RC (2007) Monte Carlo simulation of scattered and thermal photoneutron fluences inside a radiotherapy room. *Radiat Prot Dosimetry,* **123:** 56-61.
18. Garnica-Garza HM (2005) Characteristics of the photoneutron contamination present in a high-energy radiotherapy treatment room. *Phys Med Biol, 50: 531-539.*
19. LANL (Los Alamos National Laboratory) ((2002Monte

Carlo N-Particle transport Code system for Multiparticle and High Energy Applications version 2.4.0 .

20. National Council on Radiation Protection and Measurements, ((2003NCRP No.144.Radiation Protection for Particle Accelerator Facilities .

21. Mesbahi A, Fix M, Allahverdi M, Grein E, Garaati H (2005) Monte Carlo calculation of Varian 2300C/D Linac photon beam characteristics: a comparison between MCNP4C, GEANT3 and measurements. *Appl Radiat Isot*, **62:** *469-477.*

22. Mesbahi A, Reilly AJ, Thwaites DI (2006) Development and commissioning of a Monte Carlo photon beam model for Varian Clinac 2100EX linear accelerator. *Appl Radiat Isot*, **64:** *656-662.*

23. Mesbahi A (2007) Dosimetric characteristics of unflattened 6 MV photon beams of a clinical linear accelerator: A Monte Carlo study. *Appl Radiat Isot*, **65:** *1029-1036.*

24. Pena J, Franco L, Gomez F, Iglesias A, Pardo J, Pombar M (2005) Monte Carlo study of Siemens PRIMUS photoneutron production. *Phys Med Biol*, **50:** *5921-5933.*

25. Mesbahi A, Ghiasi H, Mahdavi SR (2010) Photoneutron and capture gamma dose equivalent for different room and maze layouts in radiation therapy. *Radiat Prot Dosimetry*, **140:** *242-249.*

26. International Atomic Energy Agency (IAEA) .(2006) *Radiation protection in the design of radiotherapy facilities*. Safety Reports series No. 47 (Vienna: IAEA) .

27. McGinley PH and Landry JC (1989) Neutron contamina-

tion of X-ray beams produced by the Varian Clinac 1800. *Phys Med Biol*, **34:** *777-783.*

28. Mesbahi A, Mehnati P, Keshtkar A, Farajollahi A (2007) Dosimetric properties of a flattening filter-free 6-MV photon beam: a Monte Carlo study. *Radiat Med*, **25:** *315-324.*

29. Followill DS, Stovall MS, Kry SF, Ibbott GS (2003) Neutron source strength measurements for Varian, Siemens, Elekta, and General Electric linear accelerators. *J Appl Clin Med Phys*, **4:** *189-194.*

30. Zabihzadeh M, Ay MR, Allahverdi M, Mesbahi A, Mahdavi SR, Shahriari M (2009) Monte Carlo estimation of photoneutrons contamination from high-energy X-ray medical accelerators in treatment room and maze: a simplified m:odel. *Radiat Prot Dosimetry*, **135:** *21-32.*

31. Sohrabi M and Mostofizadeh A (1999) Measurement of photoneutron doses in and out of high-energy X-ray beam of a saturne-20 medical linear accelerator by ECE polycarbonate detectors. *Radiation Measurements*, **31:** *479-482.*

32. Ghavami SM, Mesbahi A, Mohammadi E (2009) The impact of automatic wedge filter on photoneutron and photon spectra of an 18-MV photon beam. *Radiat Prot Dosimetry*, *.128-123* **: 132**

33. Mesbahi A, Keshtkar A, Mohammadi E, Mohammadzadeh M (2010) Effect of wedge filter and field size on photoneutron dose equivalent for an 18MV photon beam of a medical linear accelerator. *Appl Radiat Isot*, **68:** *84-89.*